Research Article | Vol. 28, No. 3 / 3 February 2020 / Optics Express 2714
Optics EXPRESS

Chip-based soliton microcomb module using a hybrid semiconductor laser

ARSLAN S. RAJA,[1,5] JUNQIU LIU,[1,5] NICOLAS VOLET,[2,4] RUI NING WANG,[1] JIJUN HE,[1] ERWAN LUCAS,[1] ROMAIN BOUCHANDAND,[1] PAUL MORTON,[3] JOHN BOWERS,[2] AND TOBIAS J. KIPPENBERG[1,*]

[1]*Swiss Federal Institute of Technology Lausanne (EPFL), CH-1015 Lausanne, Switzerland*
[2]*University of California, Santa Barbara (UCSB), CA 93106, USA*
[3]*Morton Photonics, West Friendship, MD 21794, USA*
[4]*Aarhus University, 8200 Aarhus N, Denmark*
[5]*These authors contributed equally to this work*
[*]*tobias.kippenberg@epfl.ch*

Abstract: Photonic chip-based soliton microcombs have shown rapid progress and have already been used in many system-level applications. There has been substantial progress in realizing soliton microcombs that rely on compact laser sources, culminating in devices that only utilize a semiconductor gain chip or a self-injection-locked laser diode as the pump source. However, generating single solitons with electronically detectable repetition rates from a compact laser module has remained challenging. Here we demonstrate a current-initiated, Si_3N_4 chip-based, 99-GHz soliton microcomb driven directly by a compact, semiconductor-based laser. This approach does not require any complex soliton tuning techniques, and single solitons can be accessed by tuning the laser current. Further, we demonstrate a generic, simple, yet reliable, packaging technique to facilitate the fiber-chip interface, which allows building a compact soliton microcomb package that can benefit from the fiber systems operating at high power (> 100 mW). Both techniques can exert immediate impact on chip-based nonlinear photonic applications that require high input power, high output power, and interfacing chip-based devices to mature fiber systems.

1. Introduction

Optical frequency combs have made significant scientific and technological advancements in the field of frequency metrology and spectroscopy [1]. Microcombs [2] allow frequency combs generated in optical microresonators with broad bandwidth, low power consumption, and repetition rates in the GHz to THz range. These microcombs have developed into an active interdisciplinary area covering frequency metrology, integrated photonics, and nonlinear soliton dynamics, and are compatible with wafer-scale manufacture and on-chip applications. Dissipative Kerr solitons (DKS), which constitute of continuously circulating ultrashort pulses in a microresonator, offer broadband and fully coherent microcombs [3]. Applications such as coherent communication [4], dual-comb spectroscopy [5], astrophysical spectrometer calibration [6,7], ultrafast distance measurement [8,9], and low-noise microwave synthesis [10,11], have been demonstrated utilizing DKS. One challenge to realize a fully integrated soliton microcomb is to combine a high-Q integrated microresonator (e.g. Si_3N_4) and a high-power laser, in order to avoid the use of external amplifiers to meet the power requirements for soliton generation. Moreover, complex soliton tuning mechanisms [12–14] to overcome the thermal effects should be avoided.

Recently, electrically driven soliton microcombs using chip-based Si_3N_4 microresonators have been demonstrated [15,16]. Despite the compact form, the lasers used in those works

#380099 https://doi.org/10.1364/OE.28.002714
Journal © 2020 Received 11 Oct 2019; revised 1 Dec 2019; accepted 2 Dec 2019; published 21 Jan 2020

Optics EXPRESS

have limited output power below 50 mW (single-mode). Nevertheless, benefitting from the advances of ultralow-loss Si_3N_4 waveguide fabrication process [17] and state-of-art high-Q Si_3N_4 microresonators [18], single soliton states with repetition rates exceeding 100 GHz were successfully demonstrated. It should be noted that, for practical applications using soliton microcombs, soliton pulses at electronically detectable repetition rates, with average pulse power more than 1 mW, are still preferred, while the aforementioned approaches suffer from limited input power from the chip laser, and the resulting low comb tooth power and high soliton repetition rate beyond what common electronic devices can detect and process. At the same time, recent reports show that packaged, semiconductor-based, fiber-coupled lasers [19] can provide sufficient output power and frequency stability for soliton microcomb generation in silica microdisks [20]. Though fragile tapered fibers to couple the silica microdisks are still required, the hybrid semiconductor lasers with high output power (~100 mW) are a promising component to build compact, portable soliton microcomb devices for practical applications that require high soliton power. In addition, this hybrid semiconductor laser features excellent noise properties, with low relative intensity noise and narrow linewidth [19]. Considering the recent demonstration of integrated Si_3N_4 soliton microcombs operating in the microwave K- and X-band at an on-chip optical power of ~ 38 mW [11], which require low-noise pump laser for low phase noise, soliton-based microwave synthesis, semiconductor lasers can potentially be a key building block for integrated soliton-based microwave photonics.

Here, we implement two solutions for compact, portable chip-based soliton microcomb devices for practical applications that require high soliton comb power per line (>15 μW) needed to amplify light while maintaining OSNR [4]. The first solution uses a commercially available hybrid semiconductor-based laser [19] to drive the Si_3N_4 chips and generate soliton microcombs of 99 GHz repetition rate. The high laser output power ~ 100 mW enables average soliton power exceeding 600 μW in the bus waveguide. Further beyond the power level of this hybrid laser, we propose an alternative solution of photonic packaging, which allows integration of chip devices into standard fiber systems operating with high power above 1 W, with significantly reduced complexity in terms of interfacing chip devices with fibers. Despite the recent advances on integrated silicon-based lasers [21] as well as the hybrid lasers used in this work, Si_3N_4 soliton microcomb chip devices still prefer to work with high input power (>100 mW), which allows, e.g. accessing integrated soliton pulses at microwave repetition rates for K- and X-band microwave synthesis [11]. Such high power currently can be offered easily by fiber laser systems with optical amplifiers (e.g. EDFA), therefore our packaging solution allows interfacing the chip devices to fiber systems. Furthermore, this packaging technique can also be applied for other integrated platforms such as AlN and $LiNbO_3$, which typically require high input power for targeted photonic applications.

2. Experiment and chip design

The Si_3N_4 microresonator chips used in this work were fabricated using the photonic Damascene reflow process [22], and feature microresonator Q-factors exceeding 1.5×10^7 across the telecom C- and L-band [18]. Key steps to achieve such high-Q include waveguide preform reflow to reduce scattering losses [23], and thorough thermal annealing to reduce hydrogen absorption losses [18]. On the Si_3N_4 chip, the microresonator is coupled to a bus waveguide, and both waveguides are 1.50 μm wide and 700 nm high, to achieve high coupling ideality [24]. Light is coupled into and out of the Si_3N_4 bus waveguide via double-inverse tapers on the chip facets [25], with >25% total coupling efficiently (fiber-chip-fiber). A polarization controller is used to align the polarization of incoming light to the transverse-electric (TE) mode. The Si_3N_4 chips were characterized using a diode laser spectroscopy technique [26,27] calibrated by a fully stabilized commercial optical frequency comb system. Each resonance was fitted [28] to extract the intrinsic linewidth $\kappa_0/2\pi$, coupling strength $\kappa_{ex}/2\pi$, and backscattering rate $\gamma/2\pi$.

Optics EXPRESS

First, we use the semiconductor laser to directly couple to the Si_3N_4 chip, as shown in Fig. 1, without using an EDFA. The laser shown in Fig. 1(b), consists of two parts. The first part is a semiconductor-based gain chip which facilitates high power operation. It features a highly reflective facet on one side and an angled facet on the other side for out-coupling [19]. The second part is a customized fiber Bragg grating (FBG) that supports single frequency and narrow linewidth operation. The light from the gain chip is coupled efficiently to the FBG via a polarization-maintaining (PM) lensed fiber. The laser power and frequency can be tuned via current control applied on the gain chip, and temperature control applied either on the gain chip or on the FBG. The maximum laser output power is around 100 mW. The laser center frequency is approximately 193.4 THz and has a tuning range of ~ 100 GHz. An isolator is used at laser output to avoid back reflection into the laser. Light coupling to the Si_3N_4 bus waveguide via optical fibers impacts the phase-difference between the pumped and the back-reflected (feedback due to intrinsic scattering) light, and leads to unstable operation. This resonant feedback has been recently used in chip-based microcomb systems to access the soliton [15,16,29]. Moreover, a single soliton generation requires a large detuning from the pump laser, which is difficult to achieve, and critically depends on the backscattered light and phase difference [30]. While the current method does not require precise control and a single soliton can be accessed deterministically via current tuning.

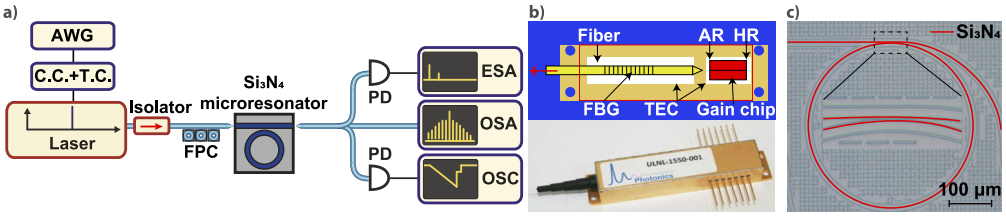

Fig. 1. Experimental setup for soliton microcomb generation using the semiconductor laser. (a) The semiconductor laser is coupled to a Si_3N_4 microresonator chip. The laser is operated via a current and a temperature controller (C.C. and T.C.). An arbitrary waveform generator (AWG) is used to scan the laser frequency over the resonance by directly modulating the laser current. The generated soliton microcomb spectrum is analysed by an optical spectrum analyser (OSA) and an electrical spectrum analyser (ESA), respectively. OSC: Oscilloscope. FPC: Fiber polarization controller. (b) A butterfly packaged semiconductor laser (bottom panel). The semiconductor laser consists of a gain chip, a FBG, and an external fiber cavity (top panel). AR: Anti-reflective coating. HR: Highly reflective coating. TEC: Thermoelectric cooler. (c) A microscope image showing a Si_3N_4 integrated microresonator, with the coupling section highlighted. The bus waveguide and microresonator are red-shaded.

The laser frequency is tuned into a microresonator resonance, by controlling the FBG temperature in small steps, until a full resonance profile is observed on the microresonator transmission spectrum. Then, the laser power is increased by actuating the current (~ 300 mA) applied on the gain chip, until a step-like pattern, signalling the soliton formation, is observed in the transmission signal. As the laser frequency changes simultaneously with the output power change due to the current increase, the FBG temperature is controlled accordingly for the laser frequency to remain on resonance. Benefit from the high microresonator Q and reduced thermal effect in Si_3N_4, the single soliton state is initiated deterministically via current tuning of the gain chip, which significantly reduces the system complexity compared with other soliton tuning techniques using “power kicking” [12], single sideband modulator [13] and dual lasers [14]. In the present work, the soliton state is generated by the simpler forward laser frequency tuning method [3]. Conventionally, a triangular shape voltage signal is applied to the laser piezo to scan over the resonance. However, laser frequency tuning is limited by the piezo scan speed. Here,

Optics EXPRESS

we directly modulate the current applied to the gain chip, allowing fast scan over resonance at kHz rate, which in turn modulates the laser frequency and power for soliton tuning and needed switching. The soliton existence range is sufficiently long, as shown in Fig. 2(d), due to the high Q-factor and the reduced thermal effects, therefore simultaneous modulation of laser frequency and power does not add extra complexity to soliton tuning. The reason is that, as the soliton exists on the effectively red-detuned side, current increase applied to the gain chip leads to an increase in the laser wavelength as well as the optical power, while the input power increase can increase the soliton existence range. A baseband radio-frequency (RF) spectrum, shown in Fig. 2(a) inset, is recorded to verify the coherence of different comb states. A modulation instability (MI) comb state is generated initially by adjusting the end point of the voltage scan signal which modulates the laser current. Then, a multi-soliton state is initiated by increasing the current and performing a scan over resonance from the blue-detuned to the red-detuned side. A low intensity noise is observed on the electrical spectrum analyser (ESA), indicating the coherent nature of the soliton state. Once all parameters are known such as the current applied to the gain chip, and the temperatures of the gain chip and the FBG, a soliton can be generated deterministically by performing an optimized current scan, which significantly simplifies the soliton initiation process. Heterodyne beatnote measurements are carried out to further confirm the intrinsic coherence of the soliton state. A narrow-linewidth (~ 10 kHz) reference laser is used to generate a beatnote with a comb tooth. The measured beatnote is fitted with a Voigt profile, and shows a Lorentzian linewidth of 9 kHz and a Gaussian linewidth of 61 kHz, as shown in Fig. 2(e). The linewidth is likely limited by the current and the temperature fluctuations of the laser driver as the main contribution in beatnote comes from Gaussian lineshape (flicker noise). The single soliton spectrum is fitted with a hyperbolic secant squared (sech^2) function, showing a pulse duration of 131-fs and a 3-dB bandwidth of 19 nm.

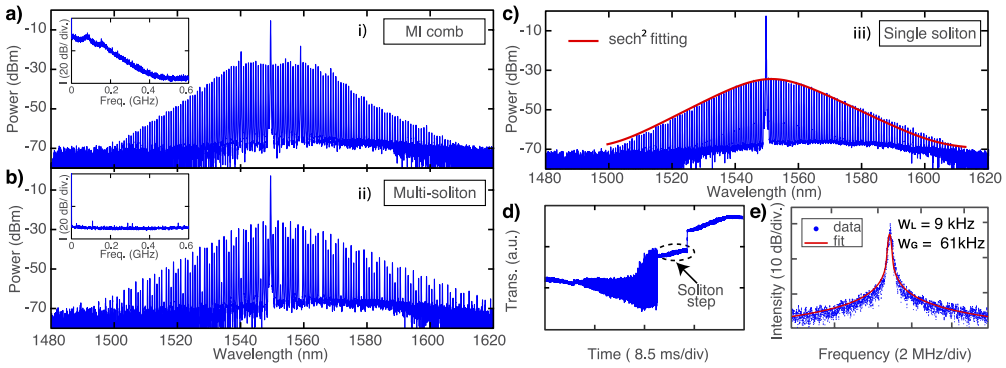

Fig. 2. Different microcomb states of 99 GHz repetition rate in a Si_3N_4 microresonator driven by the semiconductor laser. (a) An MI comb is generated by modulating the current applied to the laser gain chip. By optimizing the scan end point, a low-noise multi-soliton state (b) and a single soliton state (c) are generated. A low RF spectrum is recorded to access the coherence properties of different comb states (inset (a) and (b)). The single soliton state (iii) with a characteristic $\mathrm{sech}^2(f)$ profile, features a 3-dB bandwidth of 19 nm and a pulse duration of 131-fs. (d) Microresonator transmission signal shows a typical soliton step. The soliton is initiated by scanning the laser frequency over a microresonator resonance from the effective blue-detuned side to the red-detuned side. (e) Heterodyne beatnote signal fitted with a Voigt profile is showing a Lorentzian linewidth of 9 kHz and a Gaussian linewidth of 61 kHz.

Optics EXPRESS

3. Optical packaging

Silicon nitride microresonators fabricated using other processes which do not feature high-Q as the ones shown here, or high-Q microresonators with lower FSR, may still require high input power well above 100 mW. Meanwhile, waveguides and microresonators based on other material platforms such as $LiNbO_3$ [31,32] and AlN [33] show rich nonlinear physics and can be used to build integrated electro-optic modulators [34], which is challenging to achieve on Si_3N_4 due to the absence of effective χ^2 nonlinearity. However, compared with Si_3N_4, these waveguide platforms typically have much higher loss (lower microresonator Q) due to the fabrication constraint, thus again high power is needed to induce prominent nonlinear processes based on these platforms. Here, in addition to the previous solution of using the high-power semiconductor laser, we also implement a generic, robust packaging technique to build a compact module for chip-based nonlinear photonics e.g. soliton microcombs. The critical feature that distinguishes our packaging technique from other solutions is the high-power handling capability, which is central for soliton microcomb generation. To the best of our knowledge, such a high-power packaging solution or similar ones has been largely unexplored in the past, due to the strict misalignment tolerance (< 1 μm) and high-power operation (> 150 mW) [35]. Again, here we demonstrate with Si_3N_4 chips as an example. A 2-cm-long ultrahigh-numerical-aperture (UHNA) fiber of ~ 4.1 μm mode field diameter is used to mode-match the fiber mode to the inverse taper's mode on the Si_3N_4 chip facet, and is spliced with an SMF-28 fiber with ~ 1 dB splicing loss (Fig. 3(a), top inset) [36]. Fiber-chip-fiber through coupling efficiency of 15% is achieved using the UHNA fiber (including the splicing loss). The splicing loss is minimized by performing a multiple arc discharge which allows the UHNA fiber core to expand for adiabatic mode conversion. The fiber is aligned to the chip input facet mechanically, and then a drop of epoxy is dispensed on the fiber-chip interface using an accurate pneumatic valve. One important aspect of the packaging is to keep the initial drop size as small as possible (Fig. 3(a), inset), to avoid extra loss due to dimensional changes which occur during the glue curing. After dispensing the glue, UV curing is performed in 3 steps with different UV light intensity for optimal curing performance: 100 mW/cm^2 for 0.5 - 1 min, 200 mW/cm^2 for 1 - 3 min and 300 mW/cm^2 for 3 - 5 min. After UV curing, the packaged device is tested for long-term stability with input laser power below 1 mW. The coupling remains stable for more than 30 hours, showing the robustness of the packaged device (Fig. 3(c)). Afterwards, the input power is increased in order to generate a microcomb in the Si_3N_4 chip. Due to the higher coupling loss as compared to the case using lensed fibers, only MI comb states can be generated in the packaged device when using the semiconductor laser. The coupling losses can be reduced by packaging with lensed fibers or optimizing the inverse taper for improved mode match [37].

To demonstrate the fact that the packaged device can generate a single soliton, a different diode laser (Toptica CTL), along with an EDFA to amplify the power to overcome the coupling and the splicing losses, is used. A single soliton state is accessed in the packaged 99-GHz-FSR microresonator with an input power exceeding 150 mW (Fig. 3(d)). The packaged device can be operated in the single soliton state for few hours without any active stabilization (Fig. 3(e)). The performance of our packaging technique at high power is characterized by packaging UHNA fibers to a straight Si_3N_4 waveguide with a coupling efficiency of 19 %. At an input power of 700 mW, the out coupled light from the packaged chip remains nearly unchanged for more than 6 hours (Fig. 3(b)), showing a good power handling capability and allowing direct interfacing of chip devices to high-power fiber systems. Indeed, a similar packaged chip is used in a recent experiment which demonstrates backward stimulated Brillouin scattering in Si_3N_4 waveguides [38]. The input optical power is more than 230 mW, and no prominent fiber-chip coupling degradation is observed through the entire experiment.

Optics EXPRESS

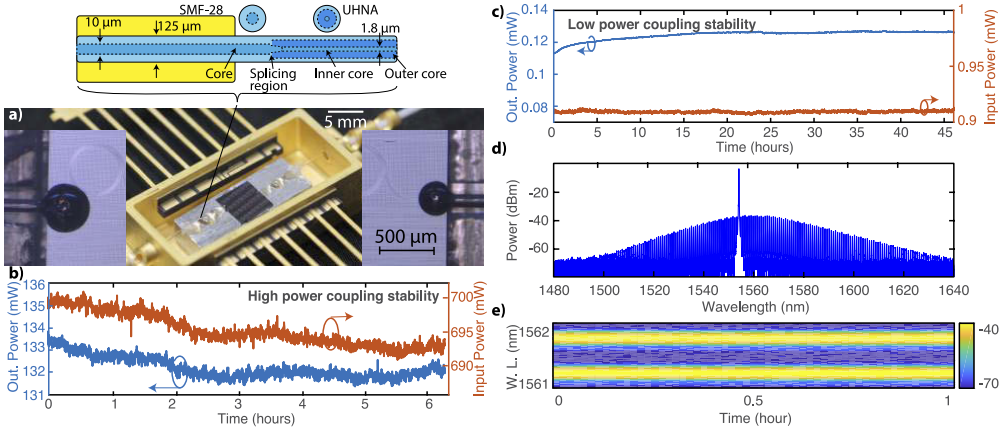

Fig. 3. Compact photonic packaging technique and its demonstration on Si_3N_4 microresonator chips for soliton microcomb generation. (a) Photonic package of a Si_3N_4 chip using an ultrahigh-numerical-aperture (UHNA) fiber spliced with an SMF-28 (top inset) inside a butterfly package. Insets: Zoom-in view of the fiber-chip facet showing the epoxy drop attach the fiber. A low-shrinkage and medium viscous epoxy has been used to minimize losses (EPO-TEK OG154). (b) The packaged device shows good power coupling stability at high power ~ 700 mW for more than 6 hours, without any active stabilization. (c) Long-term coupling performance of the packaged system. The slow increase in the output power during the initial 5 to 7 hours may be associated with the epoxy curing, which usually takes 24 hours to settle down after UV curing. (d) Single soliton generation using the Toptica laser in a packaged device. (e) A long-term stability test in the packaged system showing two lines of a single soliton microcomb (spectrum in d). The soliton state was maintained for more than one hour without any active temperature stabilization (i.e. fully free running). W. L.: Wavelength.

4. Conclusion

In summary, we have demonstrated a soliton microcomb operating at 99 GHz repetition rate directly driven by a hybrid semiconductor-based laser with high output power. The single soliton state is initiated deterministically via laser current tuning. In addition, to benefit from the high power operation of fiber systems, we demonstrate a generic photonic packaging approach which can significantly simplify the fiber-chip interface connection, and facilitates the accommodation and integration of chip-based devices into other photonic systems. We show that the packaging technique can be used to build a compact, portable microcomb system and can sustain high power operation. Also, a recent study shows that splicing loss can be minimized to less than 0.2 dB, which will improve the coupling efficiency [39]. Both approaches presented in our work can be utilized in microcomb applications requiring high power comb tooth and low soliton phase noise, such as coherent communications [4] and on-chip low-noise microwave generation [11].

Funding

Defense Advanced Research Projects Agency (HR0011-15-C- 0055); Schweizerischer Nationalfonds zur Förderung der Wissenschaftlichen Forschung (176563); H2020 European Research Council (801352); European Space Agency (4000116145/16/NL/MH/GM); Air Force Office of Scientific Research, Air Force Material Command, USAF (FA9550-19-1-0250).

Optics EXPRESS

Acknowledgments

The Si_3N_4 microresonator samples were fabricated in the EPFL center of Micro-NanoTechnology (CMi). We thank A. Lukashchuk for assistance in chip mask design. E. L. acknowledges the support from the European Space Technology Centre with ESA Contract No. 4000116145/16/NL/MH/GM.

Disclosures

The authors declare no conflicts of interest.

Data Availability Statement

The code and data used to produce the plots within this paper are available at 10.5281/zenodo.3556401. All other data used in this study are available from the corresponding authors upon reasonable request.

References

1. T. Udem, R. Holzwarth, and T. W. Hänsch, "Optical frequency metrology," Nature **416**(6877), 233–237 (2002).
2. T. J. Kippenberg, R. Holzwarth, and S. A. Diddams, "Microresonator-based optical frequency combs," Science **332**(6029), 555–559 (2011).
3. T. Herr, V. Brasch, J. D. Jost, C. Y. Wang, N. M. Kondratiev, M. L. Gorodetsky, and T. J. Kippenberg, "Temporal solitons in optical microresonators," Nat. Photonics **8**(2), 145–152 (2014).
4. P. Marin-Palomo, J. N. Kemal, M. Karpov, A. Kordts, J. Pfeifle, M. H. P. Pfeiffer, P. Trocha, S. Wolf, V. Brasch, M. H. Anderson, R. Rosenberger, K. Vijayan, W. Freude, T. J. Kippenberg, and C. Koos, "Microresonator-based solitons for massively parallel coherent optical communications," Nature **546**(7657), 274–279 (2017).
5. M.-G. Suh, Q.-F. Yang, K. Y. Yang, X. Yi, and K. J. Vahala, "Microresonator soliton dual-comb spectroscopy," Science **354**(6312), 600–603 (2016).
6. E. Obrzud, M. Rainer, A. Harutyunyan, M. H. Anderson, J. Liu, M. Geiselmann, B. Chazelas, S. Kundermann, S. Lecomte, M. Cecconi, A. Ghedina, E. Molinari, F. Pepe, F. Wildi, F. Bouchy, T. J. Kippenberg, and T. Herr, "A microphotonic astrocomb," Nat. Photonics **13**(1), 31–35 (2019).
7. M.-G. Suh, X. Yi, Y.-H. Lai, S. Leifer, I. S. Grudinin, G. Vasisht, E. C. Martin, M. P. Fitzgerald, G. Doppmann, J. Wang, D. Mawet, S. B. Papp, S. A. Diddams, C. Beichman, and K. Vahala, "Searching for exoplanets using a microresonator astrocomb," Nat. Photonics **13**(1), 25–30 (2019).
8. M.-G. Suh and K. J. Vahala, "Soliton microcomb range measurement," Science **359**(6378), 884–887 (2018).
9. P. Trocha, M. Karpov, D. Ganin, M. H. P. Pfeiffer, A. Kordts, S. Wolf, J. Krockenberger, P. Marin-Palomo, C. Weimann, S. Randel, W. Freude, T. J. Kippenberg, and C. Koos, "Ultrafast optical ranging using microresonator soliton frequency combs," Science **359**(6378), 887–891 (2018).
10. W. Liang, D. Eliyahu, V. S. Ilchenko, A. A. Savchenkov, A. B. Matsko, D. Seidel, and L. Maleki, "High spectral purity kerr frequency comb radio frequency photonic oscillator," Nat. Commun. **6**(1), 7957 (2015).
11. J. Liu, E. Lucas, J. He, A. S. Raja, R. N. Wang, M. Karpov, H. Guo, R. Bouchand, and T. J. Kippenberg, "Photonic microwave oscillators based on integrated soliton microcombs," arXiv:1901.10372 [physics] (2019).
12. V. Brasch, M. Geiselmann, M. H. P. Pfeiffer, and T. J. Kippenberg, "Bringing short-lived dissipative kerr soliton states in microresonators into a steady state," Opt. Express **24**(25), 29312–29320 (2016).
13. J. R. Stone, T. C. Briles, T. E. Drake, D. T. Spencer, D. R. Carlson, S. A. Diddams, and S. B. Papp, "Thermal and nonlinear dissipative-soliton dynamics in kerr-microresonator frequency combs," Phys. Rev. Lett. **121**(6), 063902 (2018).
14. S. Zhang, J. M. Silver, L. D. Bino, F. Copie, M. T. M. Woodley, G. N. Ghalanos, A. Ø. Svela, N. Moroney, and P. Del'Haye, "Sub-milliwatt-level microresonator solitons with extended access range using an auxiliary laser," Optica **6**(2), 206–212 (2019).
15. B. Stern, X. Ji, Y. Okawachi, A. L. Gaeta, and M. Lipson, "Battery-operated integrated frequency comb generator," Nature **562**(7727), 401–405 (2018).
16. A. S. Raja, A. S. Voloshin, H. Guo, S. E. Agafonova, J. Liu, A. S. Gorodnitskiy, M. Karpov, N. G. Pavlov, E. Lucas, R. R. Galiev, A. E. Shitikov, J. D. Jost, M. L. Gorodetsky, and T. J. Kippenberg, "Electrically pumped photonic integrated soliton microcomb," Nat. Commun. **10**(1), 680 (2019).
17. X. Ji, F. A. S. Barbosa, S. P. Roberts, A. Dutt, J. Cardenas, Y. Okawachi, A. Bryant, A. L. Gaeta, and M. Lipson, "Ultra-low-loss on-chip resonators with sub-milliwatt parametric oscillation threshold," Optica **4**(6), 619–624 (2017).
18. J. Liu, A. S. Raja, M. Karpov, B. Ghadiani, M. H. P. Pfeiffer, B. Du, N. J. Engelsen, H. Guo, M. Zervas, and T. J. Kippenberg, "Ultralow-power chip-based soliton microcombs for photonic integration," Optica **5**(10), 1347–1353 (2018).

Optics EXPRESS

19. P. A. Morton and M. J. Morton, "High-power, ultra-low noise hybrid lasers for microwave photonics and optical sensing," J. Lightwave Technol. **36**(21), 5048–5057 (2018).
20. N. Volet, X. Yi, Q.-F. Yang, E. J. Stanton, P. A. Morton, K. Y. Yang, K. J. Vahala, and J. E. Bowers, "Microresonator soliton generated directly with a diode laser," Laser Photonics Rev. **12**(5), 1700307 (2018).
21. D. Huang, M. A. Tran, J. Guo, J. Peters, T. Komljenovic, A. Malik, P. A. Morton, and J. E. Bowers, "High-power sub-khz linewidth lasers fully integrated on silicon," Optica **6**(6), 745–752 (2019).
22. M. H. P. Pfeiffer, C. Herkommer, J. Liu, T. Morais, M. Zervas, M. Geiselmann, and T. J. Kippenberg, "Photonic damascene process for low-loss, high-confinement silicon nitride waveguides," IEEE J. Sel. Top. Quantum Electron. **24**(4), 1–11 (2018).
23. M. H. P. Pfeiffer, J. Liu, A. S. Raja, T. Morais, B. Ghadiani, and T. J. Kippenberg, "Ultra-smooth silicon nitride waveguides based on the damascene reflow process: fabrication and loss origins," Optica **5**(7), 884–892 (2018).
24. M. H. P. Pfeiffer, J. Liu, M. Geiselmann, and T. J. Kippenberg, "Coupling ideality of integrated planar high-q microresonators," Phys. Rev. Appl. **7**(2), 024026 (2017).
25. J. Liu, A. S. Raja, M. H. P. Pfeiffer, C. Herkommer, H. Guo, M. Zervas, M. Geiselmann, and T. J. Kippenberg, "Double inverse nanotapers for efficient light coupling to integrated photonic devices," Opt. Lett. **43**(14), 3200–3203 (2018).
26. P. Del'Haye, O. Arcizet, M. L. Gorodetsky, R. Holzwarth, and T. J. Kippenberg, "Frequency comb assisted diode laser spectroscopy for measurement of microcavity dispersion," Nat. Photonics **3**(9), 529–533 (2009).
27. J. Liu, V. Brasch, M. H. P. Pfeiffer, A. Kordts, A. N. Kamel, H. Guo, M. Geiselmann, and T. J. Kippenberg, "Frequency-comb-assisted broadband precision spectroscopy with cascaded diode lasers," Opt. Lett. **41**(13), 3134–3137 (2016).
28. M. L. Gorodetsky, A. D. Pryamikov, and V. S. Ilchenko, "Rayleigh scattering in high-q microspheres," J. Opt. Soc. Am. B **17**(6), 1051–1057 (2000).
29. N. M. Kondratiev, V. E. Lobanov, A. V. Cherenkov, A. S. Voloshin, N. G. Pavlov, S. Koptyaev, and M. L. Gorodetsky, "Self-injection locking of a laser diode to a high-Q WGM microresonator," Opt. Express **25**(23), 28167–28178 (2017).
30. B. Shen, L. Chang, J. Liu, H. Wang, Q.-F. Yang, C. Xiang, R. N. Wang, J. He, T. Liu, W. Xie, J. Guo, D. Kinghorn, L. Wu, Q.-X. Ji, T. J. Kippenberg, K. Vahala, and J. E. Bowers, "Integrated turnkey soliton microcombs operated at cmos frequencies," arXiv **1911.02636** (2019).
31. Y. He, Q.-F. Yang, J. Ling, R. Luo, H. Liang, M. Li, B. Shen, H. Wang, K. Vahala, and Q. Lin, "A self-starting bi-chromatic linbo3 soliton microcomb," arXiv **1812.09610v1** (2018).
32. Z. Gong, X. Liu, Y. Xu, M. Xu, J. B. Surya, J. Lu, A. Bruch, C. Zou, and H. X. Tang, "Soliton microcomb generation at 2um in z-cut lithium niobate microring resonators," Opt. Lett. **44**(12), 3182–3185 (2019).
33. Z. Gong, A. Bruch, M. Shen, X. Guo, H. Jung, L. Fan, X. Liu, L. Zhang, J. Wang, J. Li, J. Yan, and H. X. Tang, "High-fidelity cavity soliton generation in crystalline aln micro-ring resonators," Opt. Lett. **43**(18), 4366–4369 (2018).
34. C. Wang, M. Zhang, M. Yu, R. Zhu, H. Hu, and M. Loncar, "Monolithic lithium niobate photonic circuits for kerr frequency comb generation and modulation," Nat. Commun. **10**(1), 978 (2019).
35. L. Carroll, J.-S. Lee, C. Scarcella, K. Gradkowski, M. Duperron, H. Lu, Y. Zhao, C. Eason, P. Morrissey, M. Rensing, S. Collins, H. Y. Hwang, and P. OBrien, "Photonic packaging: transforming silicon photonic integrated circuits into photonic devices," Appl. Sci. **6**(12), 426 (2016).
36. S. F. Preble, M. L. Fanto, J. A. Steidle, C. C. Tison, G. A. Howland, Z. Wang, and P. M. Alsing, "On-chip quantum interference from a single silicon ring-resonator source," Phys. Rev. Appl. **4**(2), 021001 (2015).
37. J. Nauriyal, M. Song, R. Yu, and J. Cardenas, "Fiber-to-chip fusion splicing for low-loss photonic packaging," Optica **6**(5), 549–552 (2019).
38. F. Gyger, J. Liu, F. Yang, J. He, A. S. Raja, R. N. Wang, S. A. Bhave, T. J. Kippenberg, and L. Thévenaz, "Observation of stimulated brillouinscattering in silicon nitride integrated waveguides," arXiv 1908.09815 (2019).
39. P. Yin, J. R. Serafini, Z. Su, R.-J. Shiue, E. Timurdogan, M. L. Fanto, M. L. Fanto, and S. Preble, "Low connector-to-connector loss through silicon photonic chips using ultra-low loss splicing of SMF-28 to high numerical aperture fibers," Opt. Express **27**(17), 24188–24193 (2019).